



HHS Public Access

Author manuscript

Int J Polym Mater. Author manuscript; available in PMC 2018 January 04.

Published in final edited form as:

Int J Polym Mater. 2017 ; 66(11): 569–576. doi:10.1080/00914037.2016.1252352.

Sequential Release of Multiple Drugs from Flexible Drug Delivery Films

Cheryl L. Jennings^a, Ellis K. Perry^a, Thomas D. Dziubla^b, and David A. Puleo^a

^aDepartment of Biomedical Engineering, University of Kentucky, Lexington, KY, USA

^bDepartment of Chemical and Materials Engineering, University of Kentucky, Lexington, KY, USA

Abstract

Sequential release of drugs aligned with the phases of tissue healing could reduce scarring. To achieve this aim, layered film devices comprising cellulose acetate phthalate (CAP) and Pluronic F-127 (Pluronic) were loaded with ketoprofen, quercetin, and pirfenidone. Citrate plasticizers were added to impart flexibility. Release of two or three drugs in sequence over several days was obtained for all multilayered devices tested. Mechanical analysis showed that elongation increased and modulus decreased with increasing plasticizer content. Release profiles can be tailored by order of layers, plasticizer concentration, and drug loaded, making CAP-Pluronic an appealing system for inhibiting scar tissue formation.

Keywords

Sequential drug release; plasticizer; drug delivery; cytotoxicity mechanical properties

Introduction

Sequential drug release is an appealing approach for targeting distinct healing phases in soft tissue defects. After hemostasis, wounds undergo inflammation that, if not controlled, can result in excessive scar tissue formation [1]. In normal healing, inflammation is a self-limiting process, and the release of inflammatory mediators, including histamine and serotonin, will decrease and cells will retract as the threat is resolved [2, 3].

During aberrant healing, chemical mediators, including arachidonic acid metabolites, cause oxidation of surrounding cells and exacerbate the inflammatory phase as proliferation begins to replace damaged tissue [4]. Within days following injury, fibroblasts migrate into the wound site, but with chronic inflammation, chemotaxis recruits excess fibroblasts to the newly forming granulation tissue [5]. Growth factors, including platelet-derived growth factor, fibroblast growth factor, and transforming growth factor- β , cause fibroblasts to

Address correspondence to: David A. Puleo, Ph.D., Department of Biomedical Engineering, University of Kentucky, 522 Robotics and Manufacturing Building, Lexington, KY 40506-0108, USA, Phone: +1-859-257-2405, Fax: +1-859-257-1856, puleo@uky.edu.

Declaration of Conflicting Interests

DAP has an equity interest in Regenera Materials, LLC, a start-up company for commercializing novel biomaterials for tissue regeneration.

differentiate into myofibroblasts that ultimately express smooth muscle actin, resulting in contractile forces in the tissue [6–9].

Current research in drug delivery has fallen short in providing systems capable of sequential delivery of multiple molecules that could be used to combat chronic inflammation and prevent fibrotic scar formation [10–17]. In most systems, drug diffuses out leaving behind the polymeric vehicle that could further inflame wounds [18–21].

The polymer films explored in this study were composed of cellulose acetate phthalate (CAP) and Pluronic F-127 (Pluronic). Together they form a complexed polymer blend that primarily releases drug as the system erodes [22–26]. Alone, CAP and Pluronic make a rigid polymer, but the addition of plasticizer imparts flexibility to the system and allows it to contour to the shape of varying wound geometries. The two plasticizers explored were citrates, namely triethyl citrate (TEC) and tributyl citrate (TBC) (Figure 1).

Three drugs were evaluated during these studies: an anti-inflammatory, ketoprofen; an anti-oxidant, quercetin; and an anti-fibrotic, pirfenidone (Figure 1). Ketoprofen non-selectively inhibits cyclooxygenase (COX) enzymes that generate proinflammatory mediators [27, 28]. Quercetin decreases superoxide activity and reduces wound contraction [29–31]. Pirfenidone reduces scar formation by down-regulating cytokines, growth factors, and cell adhesion molecules [32–34].

Sequential release of multiple drugs from plasticized CAP-Pluronic films had not been previously investigated. Layered devices were made from plasticized films loaded with ketoprofen, quercetin, or pirfenidone. The goal of these studies was to develop a mechanically flexible drug delivery system capable of sequential release that ultimately could be used to reduce fibrotic scar tissue formation as outlined in Figure 2.

Materials and Methods

Cytotoxicity Studies

C2C12 mouse myoblastic cells (CRL-1772; ATCC, Manassas, VA) were seeded into 24-well plates at a density of 15,000 cells/cm² and cultured in Dulbecco's Modified Eagle Medium (DMEM) supplemented with 10% fetal bovine serum (FBS) at 37°C in a humidified, 5% CO₂ incubator. The next day, the medium was changed, and cells were exposed for 24 hours to different concentrations of TEC or TBC plasticizer diluted into DMEM containing 10% FBS. To determine the cell viability, an MTT (3-(4, 5-dimethylthiazolyl-2)-2,5-diphenyl tetrazolium bromide; Sigma-Aldrich, St. Louis, MO) assay was performed. Three hundred μ L of 5 mg/mL MTT were added to each well and incubated for 2 hours. After replacing the medium with 500 μ L of extraction buffer composed of 20% sodium dodecyl sulfate in 50% N,N-dimethyl formamide, the plates were incubated at 37°C on an orbital shaker for 24 hr before reading absorbance at 570 nm.

Film and Device Fabrication

Polymeric films were made by combining Pluronic F-127 (Sigma-Aldrich) and cellulose acetate phthalate (CAP; Sigma-Aldrich) in a 30:70 weight ratio, respectively. Triethyl citrate

(Sigma-Aldrich) or tributyl citrate (Sigma-Aldrich) were added to the CAP and Pluronic at 0, 10, or 20 wt% to create a 2 g film. Ketoprofen (100 mg; Sigma-Aldrich), quercetin (10 mg; Sigma-Aldrich) or pirfenidone (6.13 mg; Tokyo Chemical Industries, Portland, OR) were combined with the polymers and plasticizer. A two week therapeutic dose was chosen for the ketoprofen loading, and the quercetin and pirfenidone loadings were molar equivalents at 0.033 mol. Acetone was added to make a 25% (w/v) mixture. To ensure homogeneity, the mixtures were vortexed before being poured into Teflon dishes and kept in a 10°C refrigerator overnight to let the acetone evaporate slowly.

Two different device types were made, 4- and 9-layered devices. For the 4-layered devices, films were laminated using acetone and then punched into circular discs (6 mm). Ketoprofen and pirfenidone loaded films were separated by two blank films. The discs were press-fit into polystyrene wells from a 96-well plate to ensure unidirectional erosion and release. Two device orientations were made: “forward” where the ketoprofen layer was exposed first and “reverse” where the pirfenidone layer was exposed first (Figure 3).

For the 9-layered devices, discs were cut from the films using circular punches of increasing diameter (Figure 4). The smallest layer (3.8 mm diameter), loaded with pirfenidone, was covered on either side by a blank layer of a larger diameter (5.5 mm diameter). Larger diameter quercetin-loaded layers (8 mm diameter) encased the blank layers. Another two blank layers (13.0 mm diameter) covered the quercetin layers. Ketoprofen-loaded films made up the outermost layers (18.2 mm diameter). Bonding between layers was achieved by painting acetone between films during lamination. All of the devices were desiccated for 48 hours to remove remnants acetone before analysis.

Drug Release and Erosion Studies

Four-layered devices were placed individually into glass vials with 4 mL of phosphate-buffered saline (PBS), pH 7.4. Samples were incubated at 37°C on an orbital shaker. Every 4 hours, supernatants were collected and replaced with fresh PBS. The nine-layered devices were placed into 50 mL test tubes with 30 mL of PBS. Every 12 hours, supernatants were collected and replaced with fresh PBS. Drug release at each time point was determined using high performance liquid chromatography (HPLC). HPLC analysis was performed with a Hitachi Primaide system equipped with a Kinetix C-18 column (4.6×150 mm, 5 µm; Phenomenex). For detection of ketoprofen, the mobile phase consisted of water containing 0.1% trifluoroacetic acid and acetonitrile (40:60), and UV absorbance was measured at 258 nm. For detection of pirfenidone, the mobile phase was water containing 0.2% acetic acid and acetonitrile (50:50), and measurement occurred at 310 nm. For detection of quercetin, the mobile phase consisted of water containing 2% acetic acid and acetonitrile (40:60), and UV absorbance was measured at 370 nm. Flow rates were 1 mL/min with injection volumes of 50 µl for all samples. For nondestructive erosion studies of the 9-layered devices, initial masses were measured and then every 8 hours, devices were removed from the supernatant, lightly patted dry, and weighed.

Mechanical Properties

A microtensile test die (ASTM D1708) was used to punch dog bone-shaped films that were laminated to four layers in thickness, with bonding again obtained by painting acetone between each layer. Samples were desiccated overnight before calipers were used to measure the width and thickness. Tensile testing was performed on a Bose ELF 3300 system in ramp mode with a displacement rate of 0.5 mm/sec. The elastic modulus (E), percent elongation normalized by the cross-sectional area, and ultimate tensile strength (UTS) were calculated using the sample dimensions and force and displacement data.

Statistics

Samples with the same plasticizer concentration or type were compared against each other for cytotoxicity, erosion, release, and mechanical studies. Results were analyzed using two-way ANOVA, and a p-value < 0.05 was considered statistically significant.

Results

Cytotoxicity

Triethyl citrate was significantly less toxic to C2C12 cells than was tributyl citrate at 0.5, 1, 5, and 10 $\mu\text{L/mL}$ (0.0005% to 2%) ($p < 0.001$). Background absorbance accounts for 10–20% of the baseline. Even at a low concentration, 0.5 $\mu\text{L/mL}$, TBC was found to be toxic to the cells (Figure 5). In contrast, TEC had no significant effect on cell viability at that concentration; metabolic activity was still at 96%. As the concentration of TEC increased, cell viability decreased. At 5 $\mu\text{L/mL}$ of TEC, 83% of the exposed cells were still viable, but 20 $\mu\text{L/mL}$ of TEC was found to be equally as toxic as all tested concentrations of TBC. Because of these results, all further studies were performed using only TEC-plasticized films.

Four-Layered Device Release

For the 4-layered “forward” devices, peaks of ketoprofen and pirfenidone release occurred at 4 and 16 hours, respectively, regardless of plasticizer concentration (Figure 6). The overlap of the ketoprofen and pirfenidone peaks was 12 hours for all three plasticizer concentrations. The overlapping area under the release curves, which corresponds to simultaneous release of ketoprofen and pirfenidone, was not significantly affected by the plasticizer concentration (Figure 6). The ketoprofen peaks for all three devices were also similarly shaped. One difference observed was the pirfenidone release profile for the 20 wt% TEC devices; the peak was more rounded than that for the 0 and 10 wt% TEC devices. The peak release at 16 hours was lower than that observed for the 0 and 10 wt% TEC devices, but the peaks at 12 and 20 hours were higher than those for the other two device types.

For the “reverse” devices, the peak of the first drug, pirfenidone, still occurred at 4 hours (Figure 7). However, the peak of the second drug, ketoprofen, occurred at 24 hours for 0 wt% TEC devices and at 16 hours for the plasticized devices. The release overlap of both drugs was 12 hours long for the 0 and 10 wt% TEC devices and 16 hours for the 20 wt% TEC devices. The area under the release curves was significantly different between the 20 wt% TEC devices and the 0 and 10 wt% TEC devices ($p < 0.05$) (Figure 7). The pirfenidone peak

for all three device types was similarly shaped, however the ketoprofen release profiles were all different. The 0 wt% TEC devices had a rounded release profile with similar release rates at both the 24 and 28 hour time points, whereas 10 wt% TEC devices had a more squared-shaped profile, with release occurring at 16, 20, and 24 hours being statistically the same. The 20 wt% TEC devices had a sharper release profile similar to those of the 0 and 10 wt% TEC “forward” devices.

Nine-Layered Device Release

For the 9-layered devices, peak release remained sequential except for the 20 wt% TEC devices, in which case ketoprofen and quercetin both peaked at 32 hours. Overlapping drug release was observed from the first time point with ketoprofen and quercetin (Figure 8). The ketoprofen peak was delayed with increasing plasticizer; peaks occurred at 8, 24, and 32 hours for 0, 10, and 20 wt% TEC, respectively. For all three device types, the quercetin release peak occurred at 32 hours. With increasing plasticizer concentration, the pirfenidone peak occurred earlier. The pirfenidone peak occurred at 144, 84, and 64 hours for the 0, 10, and 20 wt% TEC devices, respectively. Pirfenidone was also more quickly released with increasing plasticizer, i.e., at 96, 64, and 32 hours for 0, 10, and 20 wt% TEC devices, respectively. Peak pirfenidone release for 0 wt% TEC samples was significantly different from that for 10 and 20 wt% samples ($p < 0.05$ and $p < 0.001$, respectively). For all devices, release steadily decreased after ketoprofen and quercetin peaked, however pirfenidone rates were more sustained for the duration of the release and did not taper as did the other two drugs.

Initial water absorption increased with plasticizer content (Figure 9). Eight hours after the study began, the 20 wt% TEC devices gained 150% of their initial mass, those with 10 wt% TEC increased in mass by 38%, and 0 wt% TEC devices gained the least, with an additional 30% mass. The mass gain of the 20 wt% samples was significantly different from that of the 0 wt% samples ($p < 0.01$). The slopes of the mass loss profiles were 19, 21, and 25 mg/hr for 0, 10, and 20 wt% TEC devices, respectively. As plasticizer content increased, the mass loss profiles became less linear. The rate of mass loss from the 20 wt% samples was significantly different from that for the 0 and 10 wt% samples ($p < 0.001$ and $p < 0.05$, respectively).

Mechanical Properties

Greater amounts of plasticizer increased the elongation and decreased the ultimate tensile strength and elastic modulus of the films (Figure 10). Layered films that were not plasticized (0 wt% TEC) had a significantly higher elastic modulus and ultimate tensile strength than films that were plasticized ($p < 0.01$ and $p < 0.0001$, respectively). For elongation, every increase in plasticizer concentration was significantly different ($p < 0.05$).

Discussion

Mouse myoblastic cells were analyzed in the cytotoxicity study because they differentiate into muscle cells, which are one cell type that would be present in one potential soft tissue application of this polymeric drug delivery system. Myoblast viability was affected less by TEC than by TBC, but both plasticizers have been implicated in adverse effects on different

organ systems, including the cardiovascular, respiratory, and central nervous systems [35–37]. When taken orally, however, TEC and TBC are non-toxic even in high doses equating to 0.5 and 2 liters, respectively, in a 70 kg man [38]. Molecules delivered orally must be absorbed in the intestines, through the hepatic portal vein, and filter through the liver before circulating through the rest of the bloodstream. The mouse myoblast model examined was a worst case scenario for parenteral delivery because cell culture systems do not have a lymphatic system or blood vessels to remove the TBC or TEC, which led to the cells being unable to survive the toxic effects as concentration increased.

Both the “forward” and “reverse” four-layered devices sequentially released pirfenidone and ketoprofen. The first drug released always had a sharp peak that occurred at 4 hours, whereas the second peak was much wider than the first, regardless of drug order. It was observed that the center of the devices eroded faster than the edges, resulting in donut-shaped devices during the last few hours of release. Factors that affected the second peak and the mechanism of erosion include the geometry and material of the wells. The surface tension in the narrow cylindrical wells likely reduced movement of the supernatant during shaking. In addition, because polystyrene is a hydrophobic polymer, it can form nanobubbles on the surface that prevent complete wetting of the material closest to the walls [39]. Some small bubbles were observed on the polystyrene wells during testing (not shown). This incomplete wetting protected the edges of the films and allowed more movement of supernatant, and therefore greater polymer erosion, toward the center of the well. Consequently, the center of the last (bottom) drug-loaded layer began eroding before edges of the two blank layers separating them had completely eroded. Lastly, plasticized CAP-Pluronic films develop pores as they erode, and these pores could facilitate diffusion of the second drug, allowing it to release sooner and for a longer duration, thereby broadening its release peak [40].

The profile of the second drug released from the 0 wt% TEC “forward” and “reverse” devices was quite different. The “forward” device had a steep slope before and after the peak at 16 hours, while the “reverse” device had a much smaller slope before and after the peak. Differences in the drug properties affected the release profiles. The solubility of pirfenidone and ketoprofen in water is 4.4 mg/mL and 51 µg/mL, respectively [41, 42], and ketoprofen is also 1.37 times larger than pirfenidone. Pirfenidone as the second drug was released more easily than ketoprofen. Ketoprofen, being larger and less water soluble than pirfenidone, cannot diffuse out of the film as easily as pirfenidone. This explanation is also supported by the differences between the “forward” and “reverse” overlapping release. The “forward” 0 and 10 wt% TEC devices had larger overlaps of the two drugs than did the “reverse” devices. Plasticizer did not affect release of pirfenidone as the second drug, but it did significantly increase the release of ketoprofen from 20 wt% TEC “reverse” devices compared to the 0 and 10 wt% TEC devices.

In the 9-layered devices, the concentration of TEC affected the release profiles by altering mobility of the three drugs. Increased TEC concentrations delayed the initial release of ketoprofen but resulted in a quicker pirfenidone release. This release mechanism has been seen before in hydroxypropyl methylcellulose matrices loaded with poorly soluble drugs [43]. TEC is more water soluble than ketoprofen, 65 mg/mL and 51 µg/mL, respectively [41,

44]. Because of this, TEC diffused from the polymer system faster than ketoprofen was released. The more TEC in the device, the slower ketoprofen was released. TEC is 1.5x and 1.1x larger than pirfenidone and ketoprofen, respectively, and comparable in size to quercetin. As TEC leached out of the films, it left behind pores large enough for the drugs to diffuse out, which is why pirfenidone release occurred faster as TEC concentration increased [40, 45, 46]. This increased porosity also accounts for the mass gain measured by the 10 and 20 wt% TEC films as water entered the porous network [47].

Compared to mechanical properties of single films plasticized with TEC or TBC [40], the four-layered films elongated more and had a lower UTS and modulus. Two of the four layers contained drug. As reported previously, the drug likely acted as plasticizer to further affect mechanical properties of the films [48]. Because of the additional thickness of the four-layered films, it is also possible that the acetone used to laminate the layers was not able to completely diffuse out of the polymer within 24 hours. Any remnant acetone would further plasticize the films [49]. Because acetone is toxic, future implanted devices need to be thoroughly processed to remove residual solvent.

Conclusion

CAP-Pluronic films are surface-eroding systems capable of sequentially releasing multiple drugs over several days. Release profiles can be tailored by the order of layers, concentration of plasticizer, and the type of drug loaded into the films. This makes them to be an appealing system for flexible drug delivery films, such as for the prevention of scar tissue formation in soft tissue defects.

Acknowledgments

This research was funded by the National Institutes of Health (DE019645 and AR060964). CJ was supported by NSF IGERT (DGE-0653710).

References

1. Schreml S, et al. Wound healing in the 21st century. *Journal of the American Academy of Dermatology*. 2010; 63(5):866–881. [PubMed: 20576319]
2. Serhan CN, Savill J. Resolution of inflammation: the beginning programs the end. *Nature immunology*. 2005; 6(12):1191–1197. [PubMed: 16369558]
3. James M, et al. Eicosanoid production by human monocytes: does COX-2 contribute to a self-limiting inflammatory response? *Inflammation Research*. 2001; 50(5):249–253. [PubMed: 11409487]
4. Cotran, RS., Kumar, V., Robbins, SL. *Robbins Pathologic Basis of Disease*. 5th. W.B. Saunders Company; Philadelphia, Pennsylvania: 1994.
5. Kumar, V., Cotran, RS., Robbins, SL. *Basic Pathology*. 5th. W.B. Saunders Company; Philadelphia, Pennsylvania: 1992.
6. Gabbiani G. The myofibroblast in wound healing and fibrocontractive diseases. *J Pathol*. 2003; 200(4):500–503. [PubMed: 12845617]
7. Tomasek JJ, et al. Myofibroblasts and mechano-regulation of connective tissue remodelling. *Nature Reviews Molecular Cell Biology*. 2002; 3(5):349–363. [PubMed: 11988769]
8. Kwan P, et al. Scar and Contracture: Biological Principles. *Hand Clinics*. 2009; 25(4):511–28. [PubMed: 19801124]

9. Paz Z, Shoenfeld Y. Antifibrosis: to reverse the irreversible. *Clin Rev Allergy Immunol*. 2010; 38(2–3):276–86. [PubMed: 19548121]
10. Wood KC, et al. Tunable Drug Release from Hydrolytically Degradable Layer-by-Layer Thin Films. *Langmuir*. 2005; 21(4):1603–1609. [PubMed: 15697314]
11. Huang SJ, et al. Folate-mediated chondroitin sulfate-Pluronic 127 nanogels as a drug carrier. *Eur J Pharm Sci*. 2009; 38(1):64–73. [PubMed: 19540339]
12. Pinon-Segundo E, et al. Preparation and characterization of triclosan nanoparticles for periodontal treatment. *Int J Pharm*. 2005; 294(1–2):217–32. [PubMed: 15814246]
13. Shelke NB, Aminabhavi TM. Synthesis and characterization of novel poly(sebacic anhydride-co-Pluronic F68/F127) biopolymeric microspheres for the controlled release of nifedipine. *Int J Pharm*. 2007; 345(1–2):51–8. [PubMed: 17616283]
14. Min J, Braatz RD, Hammond PT. Tunable staged release of therapeutics from layer-by-layer coatings with clay interlayer barrier. *Biomaterials*. 2014; 35(8):2507–2517. [PubMed: 24388389]
15. Dyondi D, Webster TJ, Banerjee R. A nanoparticulate injectable hydrogel as a tissue engineering scaffold for multiple growth factor delivery for bone regeneration. *Int J Nanomedicine*. 2013; 8:47. [PubMed: 23293519]
16. Karam J-P, et al. Pharmacologically active microcarriers associated with thermosensitive hydrogel as a growth factor releasing biomimetic 3D scaffold for cardiac tissue-engineering. *Journal of Controlled Release*. 2014; 192:82–94. [PubMed: 24998940]
17. Shemesh M, et al. Controlled release of analgesic drugs from porous bioresorbable structures for various biomedical applications. *Journal of Biomaterials Science-Polymer Edition*. 2014; 25(4):410–430. [PubMed: 24313726]
18. Siepmann J, Peppas NA. Modeling of drug release from delivery systems based on hydroxypropyl methylcellulose (HPMC). *Advanced Drug Delivery Reviews*. 2012; 64(Supplement):163–174.
19. LaVan DA, McGuire T, Langer R. Small-scale systems for in vivo drug delivery. *Nat Biotech*. 2003; 21(10):1184–1191.
20. Kumari A, Yadav SK, Yadav SC. Biodegradable polymeric nanoparticles based drug delivery systems. *Colloids and Surfaces B: Biointerfaces*. 2010; 75(1):1–18. [PubMed: 19782542]
21. Aw MS. A multi-drug delivery system with sequential release using titania nanotube arrays. *Chemical communications*. 2012; 48(27):3348–3350. [PubMed: 22367413]
22. Sundararaj SC, et al. Bioerodible system for sequential release of multiple drugs. *Acta Biomaterialia*. 2014; 10(1):115–125. [PubMed: 24096151]
23. Sundararaj SC, et al. Design of a multiple drug delivery system directed at periodontitis. *Biomaterials*. 2013; 34(34):8835–8842. [PubMed: 23948165]
24. Jeon JH, Puleo DA. Alternating release of different bioactive molecules from a complexation polymer system. *Biomaterials*. 2008; 29(26):3591–3598. [PubMed: 18514812]
25. Sundararaj SC, et al. Comparison of sequential drug release in vitro and in vivo. *Journal of Biomedical Materials Research Part B: Applied Biomaterials*. 2015
26. Jennings CL, Dziubla TD, Puleo DA. Combined effects of drugs and plasticizers on the properties of drug delivery films. *Journal of Bioactive and Compatible Polymers: Biomedical Applications*. 2016; 31(4):323–333.
27. USP Veterinary Pharmaceutical Information Monographs - Anti-inflammatories. *Journal of Veterinary Pharmacology and Therapeutics*. 2004; 27:1–110.
28. Ricci M, et al. Ketoprofen controlled release from composite microcapsules for cell encapsulation: Effect on post-transplant acute inflammation. *Journal of Controlled Release*. 2005; 107(3):395–407. [PubMed: 16129507]
29. Gomathi K, et al. Quercetin incorporated collagen matrices for dermal wound healing processes in rat. *Biomaterials*. 2003; 24(16):2767–2772. [PubMed: 12711523]
30. Baowen Q, et al. A further investigation concerning correlation between anti-fibrotic effect of liposomal quercetin and inflammatory cytokines in pulmonary fibrosis. *Eur J Pharmacol*. 2010; 642(1–3):134–9. [PubMed: 20510684]
31. Hu Q, et al. In vitro anti-fibrotic activities of herbal compounds and herbs. *Nephrol Dial Transplant*. 2009; 24(10):3033–41. [PubMed: 19474275]

32. Hewitson TD, et al. Pirfenidone reduces in vitro rat renal fibroblast activation and mitogenesis. *Journal of Nephrology*. 2001; 14(6):453–460. [PubMed: 11783601]
33. Kaneko M, et al. Pirfenidone induces intercellular adhesion molecule-1 (ICAM-1) down-regulation on cultured human synovial fibroblasts. *Clinical and Experimental Immunology*. 1998; 113(1):72–76. [PubMed: 9697986]
34. Card JW, et al. Differential Effects of Pirfenidone on Acute Pulmonary Injury and Ensuing Fibrosis in the Hamster Model of Amiodarone-Induced Pulmonary Toxicity. *Toxicological Sciences*. 2003; 75(1):169–180. [PubMed: 12832656]
35. [accessed 10/17/16] Material Safety Data Sheet for Tributyl Citrate. Available from: <http://www.sciencelab.com/msds.php?msdsId=9925302>
36. Meyers DB, Autian J, Guess WL. Toxicity of plastics used in medical practice II. Toxicity of citric acid esters used as plasticizers. *Journal of Pharmaceutical Sciences*. 1964; 53(7):774–777. [PubMed: 14209477]
37. Gerhardt P. Brucella suis in Aerated Broth Culture: III. Continuous Culture Studies. *Journal of Bacteriology*. 1946; 52(3):283–292.
38. Finkelstein M, Gold H. Toxicology of the citric acid esters: Tributyl citrate, acetyl tributyl citrate, triethyl citrate, and acetyl triethyl citrate. *Toxicology and Applied Pharmacology*. 1959; 1(3):283–298. [PubMed: 13659536]
39. Simonsen AC, Hansen PL, Klösgen B. Nanobubbles give evidence of incomplete wetting at a hydrophobic interface. *Journal of Colloid and Interface Science*. 2004; 273(1):291–299. [PubMed: 15051463]
40. Rabek C, Van Stelle R, Dziubla TD, Puleo DA. The Effect of Plasticizers on the Erosion and Mechanical Properties of Polymer Films. *Journal of Biomaterials Applications*. 2014; 28(5):779–789. [PubMed: 23520360]
41. [accessed 10/17/16] Ketoprofen. Available from: <http://www.drugbank.ca/drugs/DB01009>
42. [accessed 10/17/16] Pirfenidone. Available from: <https://scifinder.cas.org/scifinder/view/scifinder/scifinderExplore.jsf>
43. Siepmann J, Peppas NA. Hydrophilic Matrices for Controlled Drug Delivery: An Improved Mathematical Model to Predict the Resulting Drug Release Kinetics (the “sequential Layer” Model). *Pharmaceutical Research*. 17(10):1290–1298.
44. [accessed 10/17/16] Triethyl Citrate. Available from: <http://www.thegoodscentscompany.com/data/rw1012771.html>
45. Klose D, et al. How porosity and size affect the drug release mechanisms from PLGA-based microparticles. *International Journal of Pharmaceutics*. 2006; 314(2):198–206. [PubMed: 16504431]
46. Berg MC, et al. Controlled Drug Release from Porous Polyelectrolyte Multilayers. *Biomacromolecules*. 2006; 7(1):357–364. [PubMed: 16398536]
47. Kabiri K, Zohuriaan-Mehr MJ. Porous Superabsorbent Hydrogel Composites: Synthesis, Morphology and Swelling Rate. *Macromolecular Materials and Engineering*. 2004; 289(7):653–661.
48. Siepmann F, Le Brun V, Siepmann J. Drugs acting as plasticizers in polymeric systems: A quantitative treatment. *Journal of Controlled Release*. 2006; 115(3):298–306. [PubMed: 17045358]
49. Paik MY, et al. Reversible Morphology Control in Block Copolymer Films via Solvent Vapor Processing: An in Situ GISAXS Study. *Macromolecules*. 2010; 43(9):4253–4260. [PubMed: 21116459]

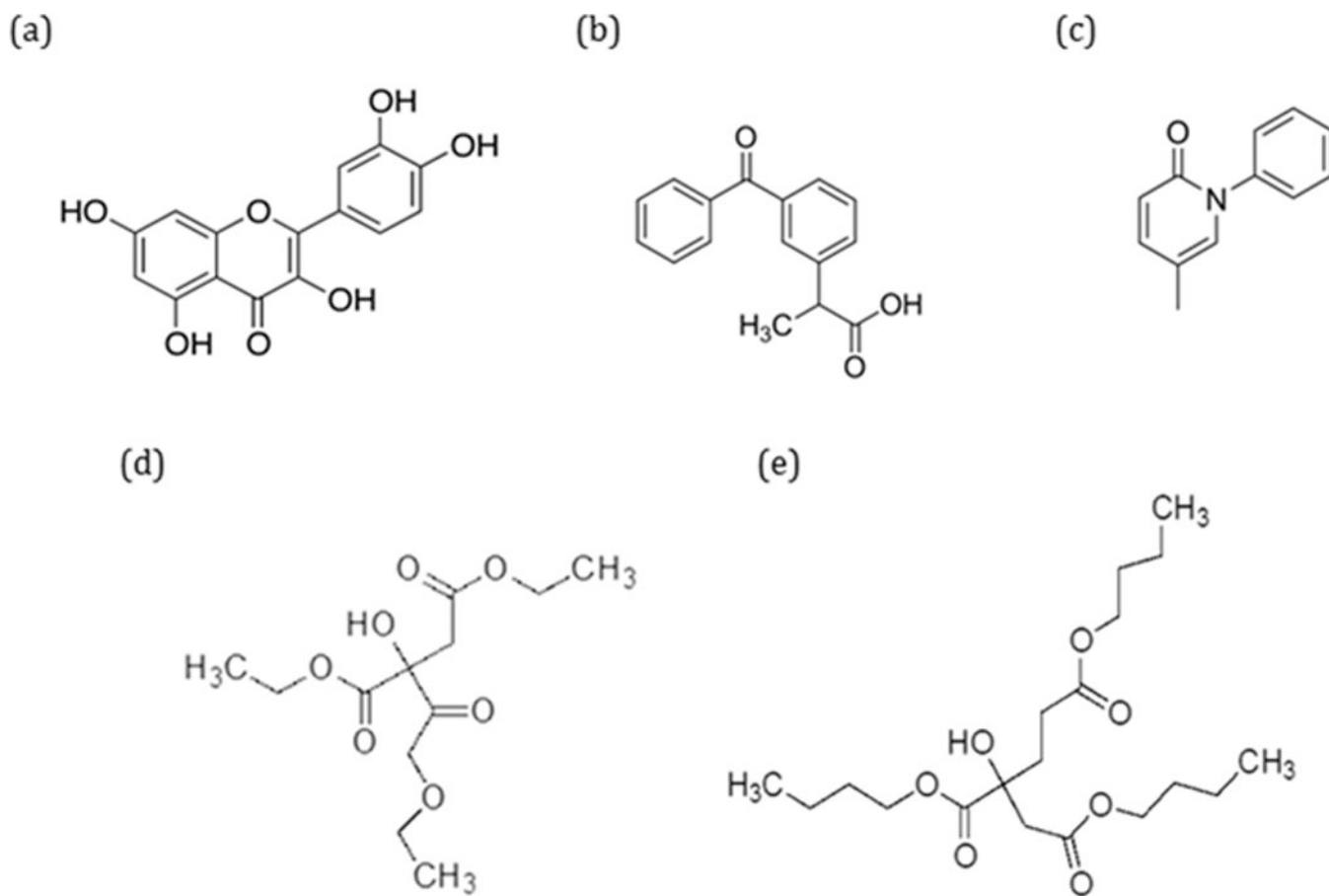


Figure 1. Chemical structures of drugs, (a) quercetin, (b) ketoprofen, and (c) pirfenidone, and plasticizers, (d) triethyl citrate and (e) tributyl citrate.

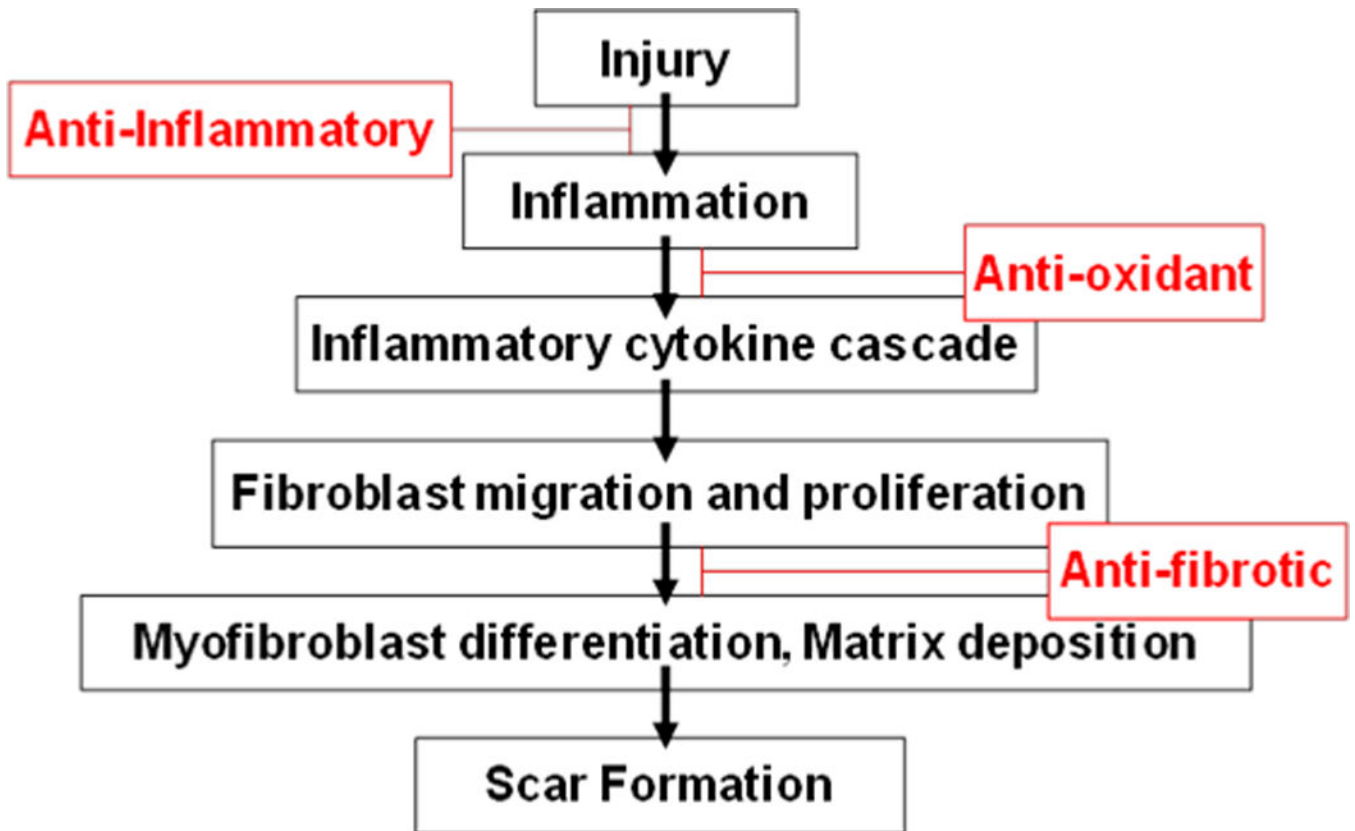


Figure 2.
Wound healing stages and the proposed drug interventions.

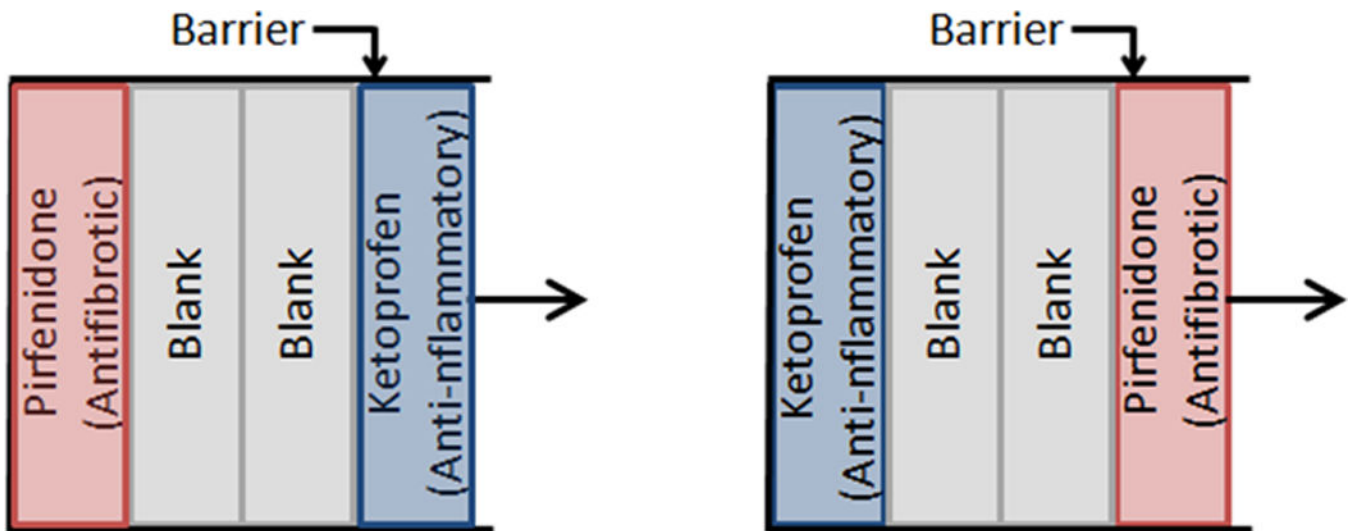


Figure 3. Schematic illustrations of 4-layered devices: (left) “forward” and (right) “reverse”.

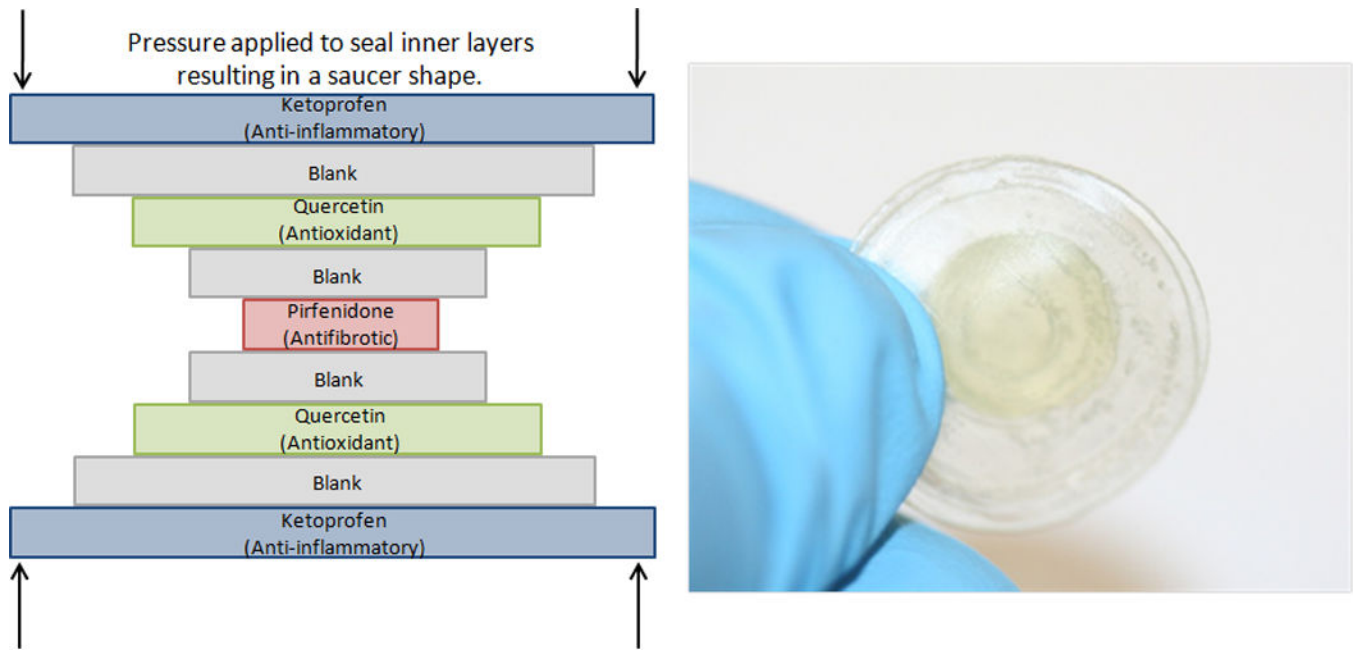


Figure 4. Schematic illustration (left) and image (right) of 9-nine layered device.

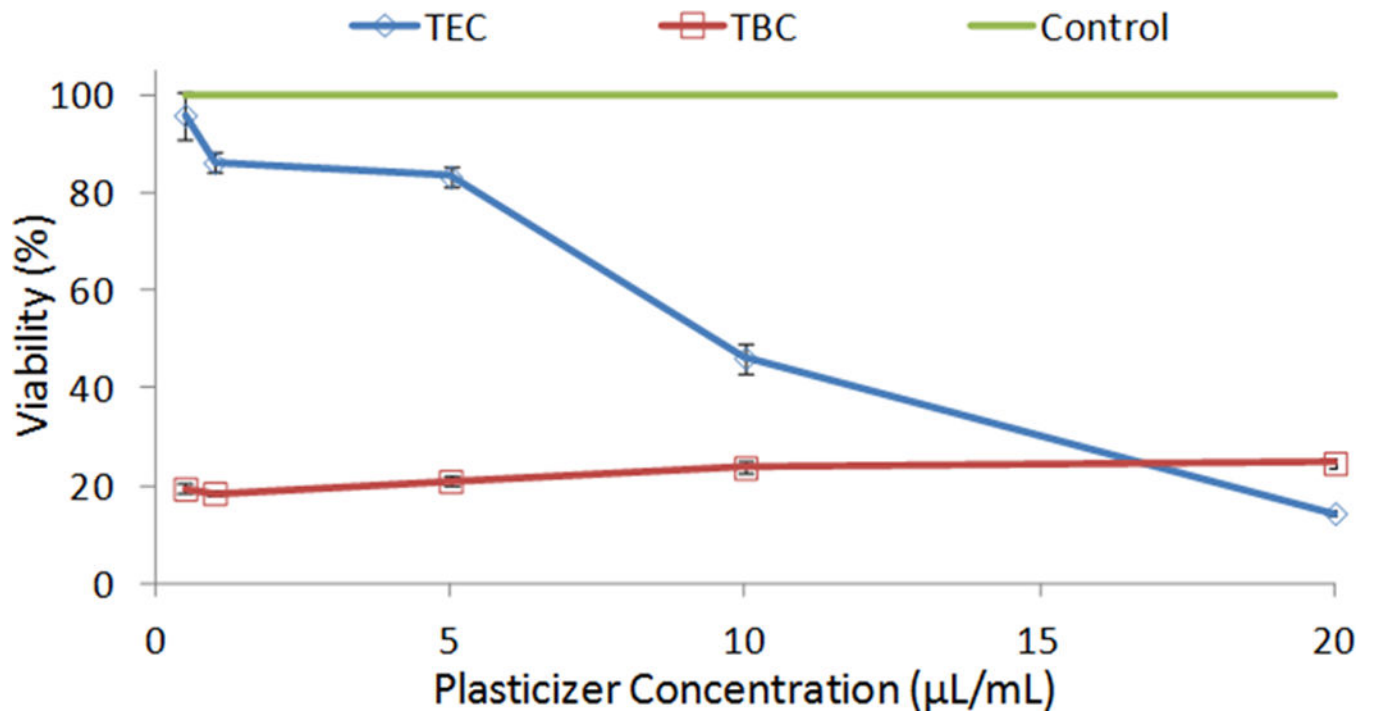


Figure 5. C2C12 myoblast viability after plasticizer exposure. Data are mean \pm standard deviation (n=3).

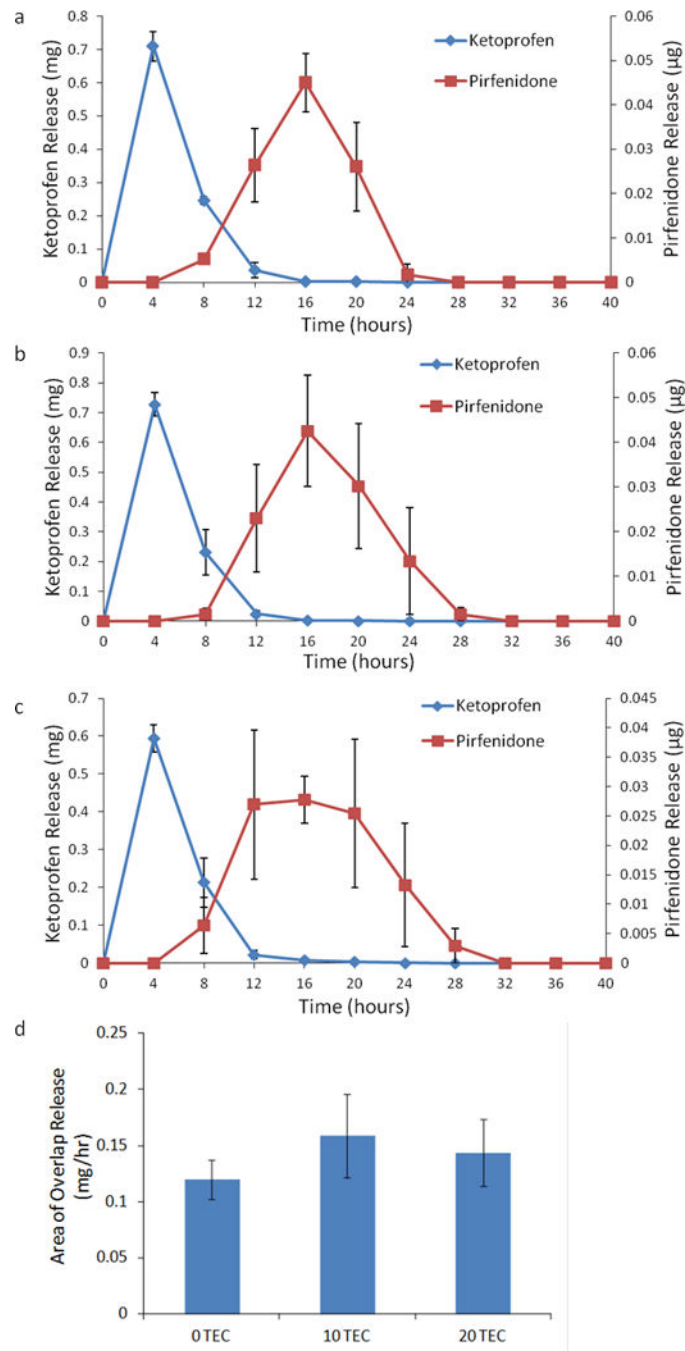


Figure 6. Release from “forward” 4-layered devices plasticized with (a) 0, (b) 10, or (c) 20 wt% TEC. (d) Overlapping area under the curves during ketoprofen and pirfenidone release. Data are mean \pm standard error ($n=3$).

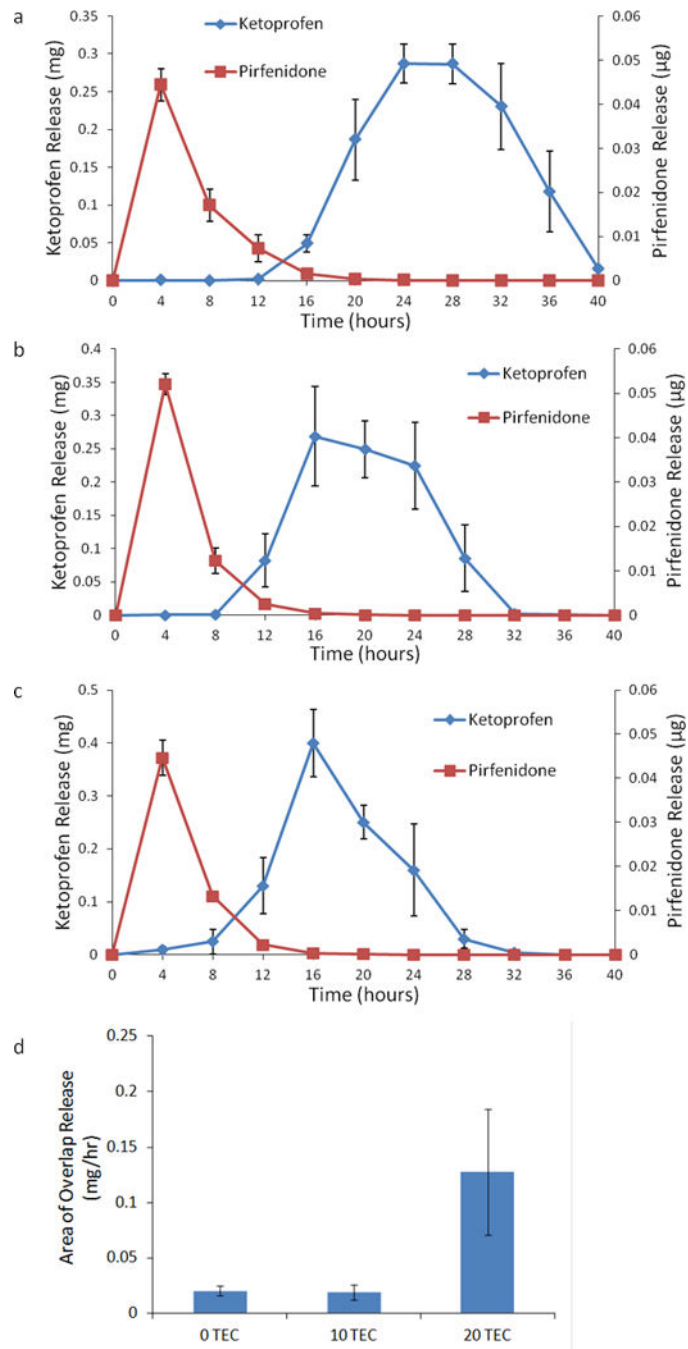


Figure 7. Release from “reverse” 4-layered devices plasticized with (a) 0, (b) 10, or (c) 20 wt% TEC. (d) Overlapping area under the curves during ketoprofen and pirfenidone release. Data are mean \pm standard error (n=3).

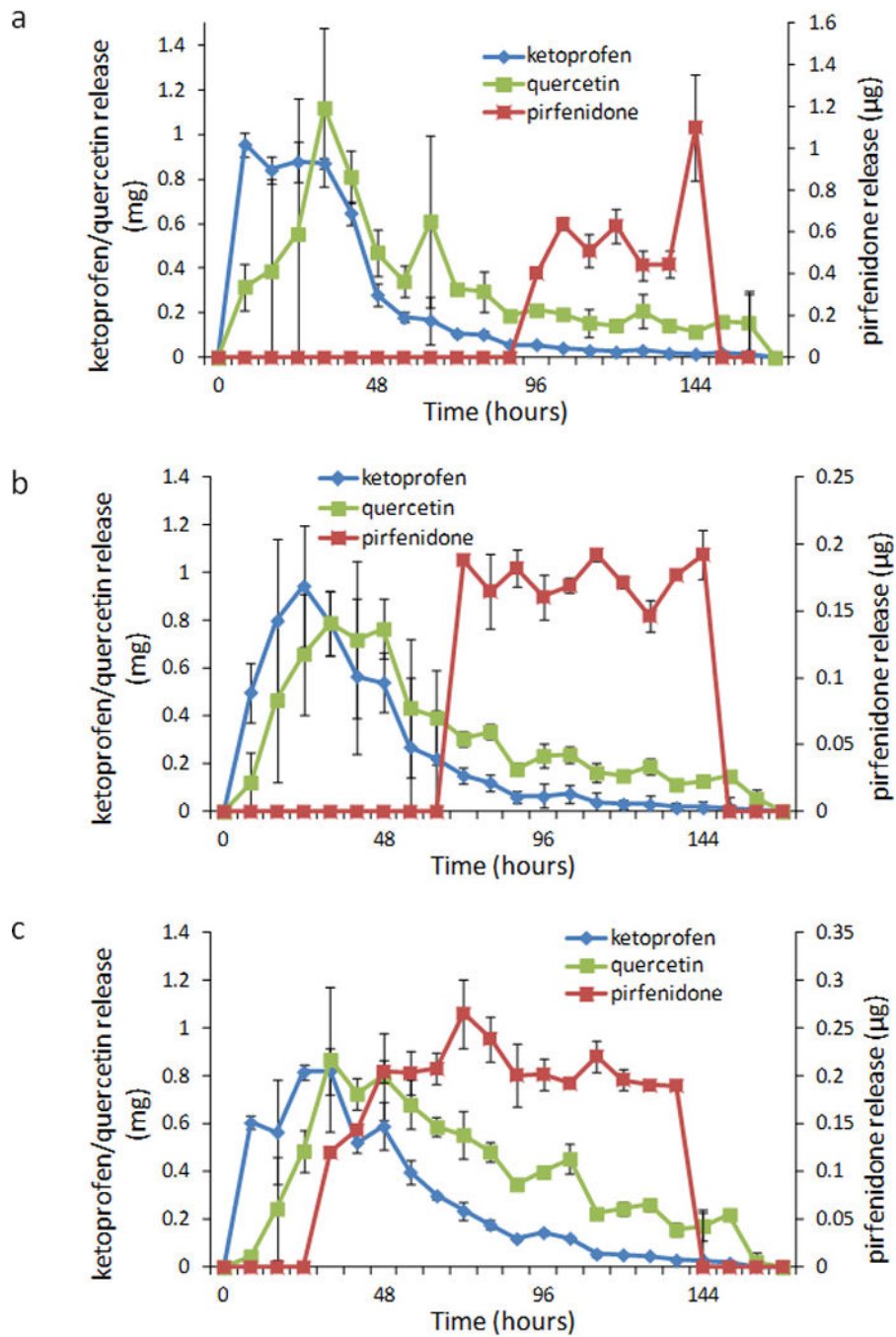


Figure 8. Release from 9-layered devices plasticized with (a) 0, (b) 10, or (c) 20 wt% TEC. Data are mean \pm standard error (n=3).

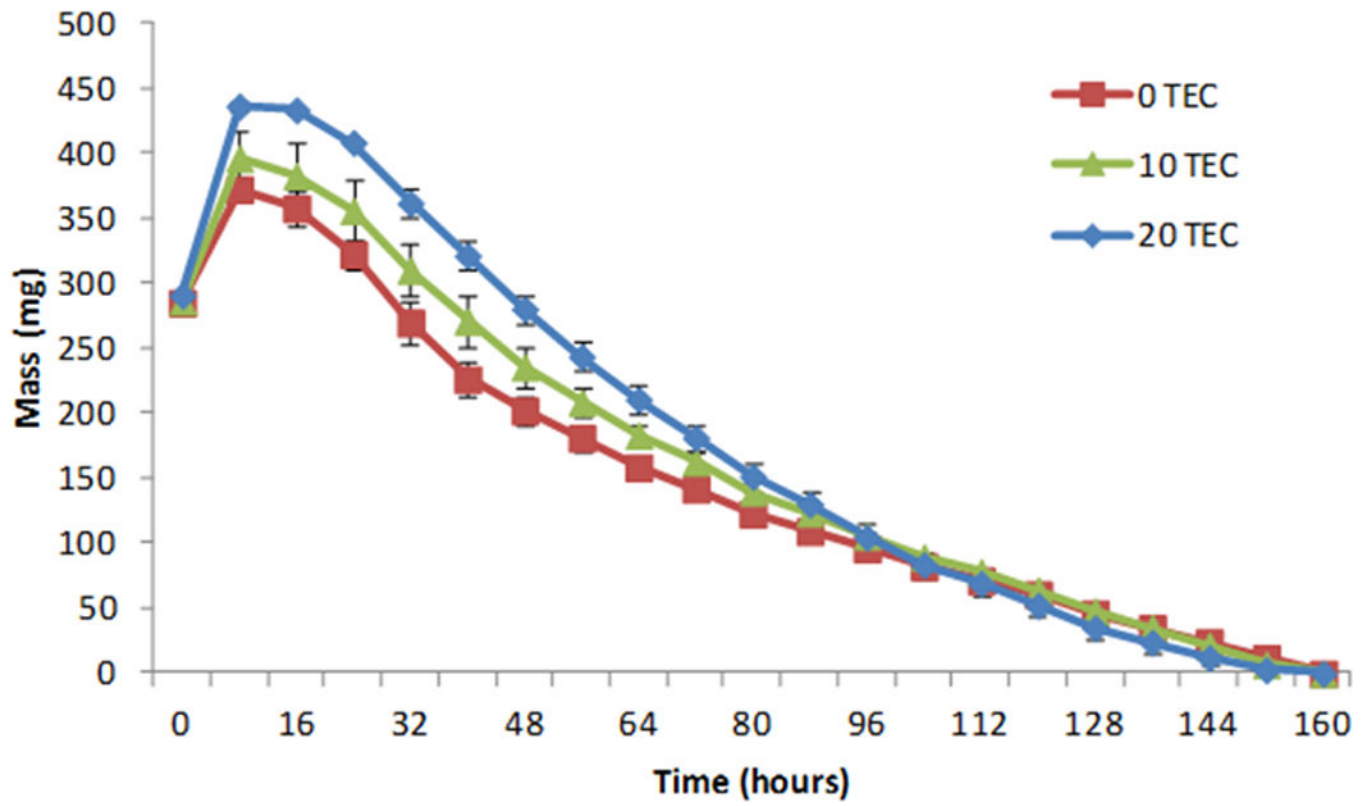


Figure 9. Mass loss of 9-layered devices. Data are mean \pm standard error (n=3).

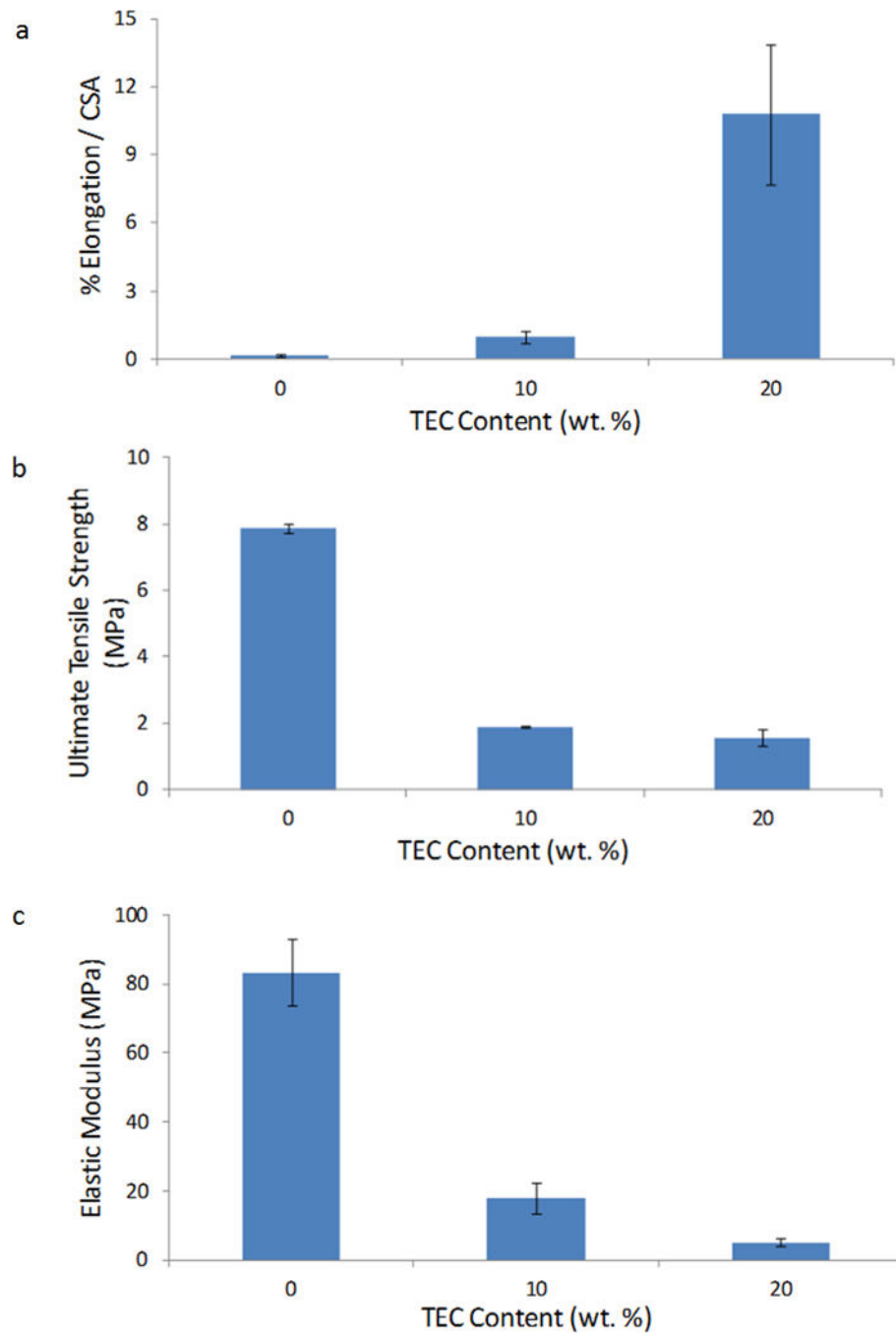


Figure 10. Mechanical properties of 4-layered devices: (a) percent elongation, (b) ultimate tensile strength, and (c) elastic modulus. Data are mean \pm standard error (n=3).